

LOW-THRUST APPROACH AND GRAVITATIONAL CAPTURE AT MERCURY

R. Jehn⁽¹⁾, S. Campagnola⁽¹⁾, D. Garcia⁽¹⁾, and S. Kemble⁽²⁾

⁽¹⁾European Space Operations Centre (ESOC),

⁽¹⁾Robert-Bosch-Str. 5, D-64293 Darmstadt, Germany, Email: Ruediger.Jehn@esa.int

⁽²⁾Astrium Ltd, Stevenage, UK

ABSTRACT

BepiColombo, an ESA science mission, will reach Mercury in early 2017. The complex nearly 5-year long transfer consists of 6 flybys and many extended thrust arcs where the spacecraft is accelerated by solar electric propulsion. The thrust level is too low for a capture from a hyperbolic approach. To avoid a single point failure of a classical chemical orbit insertion burn, a trajectory is proposed where the gravity of the Sun is exploited to weakly capture the spacecraft in a Mercury orbit. The arrival conditions are optimised taking into account the interplanetary delta-V and low-cost recovery options in case of a failed orbit insertion. Finally, the navigation aspects for this unusual approach trajectory are studied.

1. THE WEAK CAPTURE PHENOMENON

Ballistic capture, sometimes called gravitational capture or also weak stability capture was intensively studied for the Earth-Moon transfer. Belbruno and Miller's seminal work in the late eighties and early nineties [1] - [3] laid the foundation for numerous follow-on analyses. Especially the Japanese scientists studied (and later on actually used) this mechanism by which an object from outside the sphere of influence attains low relative velocity with regard to the central body and even can orbit around it temporarily [13].

An analysis of the circular, restricted three-body problem shows that motion under the influence of two gravity fields can be characterised in terms of the Jacobi constant, or 'surface of zero velocity'. An analysis of the characteristics of this constrained motion suggests the conditions for planetary approach under which gravitational perturbations may be effective in capture. This effect is observed in nature, where the phenomenon of temporary satellite capture, or transit from one heliocentric orbit to another by gravitational perturbation, has been seen for asteroids and comets.

Jupiter has been found to be responsible for numerous modifications to small body orbits in the solar system. Examination of the Jovian system and neighbouring heliocentric orbits shows many irregular bodies, some of which are likely to have been temporarily captured via approaching through the Lagrange points [7],[11],[12].

A noticeable example is Comet Shoemaker-Levy 9, which eventually impacted Jupiter in 1994.

The characteristic approach excess hyperbolic velocities, prior to temporary capture into a high elliptical orbit, can be calculated approximately for a range of planets [10]. They are shown in Table 1 for the 5 inner planets.

Table 1. Characteristic approach/departure excess hyperbolic velocities linking to high apocentre orbits.

Planet	Excess Velocity
Mercury	300 m/s
Venus	900 m/s
Earth	1000 m/s
Mars	300 m/s
Jupiter	3000 m/s

The greatest effects are seen at the outer planets, however, there are significant transfer time penalties in adopting such an approach (about half the planet's orbital period). Consequently, the technique becomes more interesting for missions to the inner planets.

ESA plans to send 'BepiColombo' to Mercury in 2012. It consists of two spacecraft: MPO (Mercury Planetary Orbiter) and MMO (Mercury Magnetospheric Orbiter), the JAXA contribution to BepiColombo. The interplanetary trajectory is already very complex with flybys at the Moon, Earth, Venus (twice) and Mercury (twice) and several low-thrust arcs of about 10 000 h in total [5]. The challenges do not stop when BepiColombo approaches Mercury in late 2016 - early 2017. The traditional chemical orbit insertion burn was considered as a single-point failure, since if the chemical engine fails to brake the hyperbolic excess velocity, the spacecraft will be kicked back into interplanetary space and the mission would be lost. There is one option with a chemical insertion burn at local noon, where a failed insertion burn could be recovered with a moderate correction manoeuvre a few days later and a new Mercury approach one Mercury year (88 days) later, however this option had to be discarded for thermal reasons [8].

Therefore, it is considered to use the solar electric propulsion module to reduce the excess velocity. However, since the thrust level is so low (about 0.4 N for a

spacecraft mass of more than 1.5 tons), an immediate capture into a stable orbit with a low perihelion altitude is not possible. The only possibility is to exploit the gravity of the Sun to get the spacecraft 'weakly captured'.

2. SCANNING THE ARRIVAL DATES

The mission analysis work performed at ESOC was to find the proper approach conditions such that the spacecraft is ballistically captured in an orbit which is stable over a few revolutions. In this case the chemical orbit insertion into the target orbit (a polar, 400 x 12000 km orbit) is allowed to fail once or even multiple times. The problem is solved by forward and backward propagation from the perihelion where the nominal orbit insertion is supposed to take place. The perihelion velocity was chosen such that the osculating apohelion altitude was between 180 000 and 200 000 km. All the other orbital elements were defined by the requirements of the BepiColombo mission [6]: 400 km perihelion altitude, 90° inclination, argument of perihelion of 178° and right ascension of ascending node of 248° (corresponding to a beta-angle of 0° required for the libration experiment [9] and for thermal reasons; β describes the orientation of the line of apsides with respect to Mercury's perihelion direction). The backward propagation shall find trajectories where the spacecraft leaves the attraction of Mercury due to the gravitational perturbations of the Sun (backward integration time of 50 days). Any backward trajectory that stays within a distance of 300 000 km to Mercury is of no use (not accessible from interplanetary space) and denoted as "incoming: closed". Trajectories that escape directly from Mercury are called "incoming: open".

Similarly, all trajectories are propagated forward to find those where the spacecraft stays within 300 000 km from Mercury for at least 50 days. These trajectories are denoted as: "outgoing: closed". If the Sun perturbations are too strong to allow for some complete orbits, we call the trajectory "outgoing: open". Fig. 1 shows the four possible combinations of incoming and outgoing trajectories as a function of the arrival time or more precisely as a function of the true anomaly of Mercury at arrival. The green part (light grey in black and white copies) shows those arrival conditions where the spacecraft approaches Mercury from infinity (speaking in mission analysis jargon) and performs some revolutions around Mercury before it possibly escapes again. As the figure shows, there are 4 more or less wide sectors with favourable arrival conditions.

The next step is to select one of the possible arrival true anomalies. In some designs of the BepiColombo spacecraft (which is currently under study), thermal analysis showed that an orbit insertion with a Mercury true anomaly between 60° and 120° (or symmetrically, between -120° and -60°) is required. Hence, this interval was scanned to find a trajectory with a low interplanetary

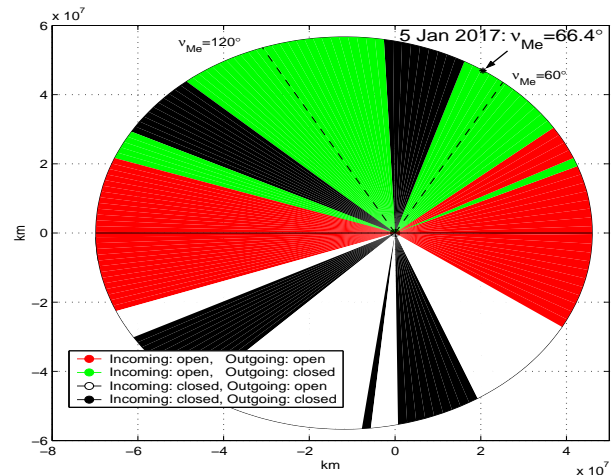


Figure 1. Mercury orbit around the Sun. The green area (light grey) indicates true anomalies where the spacecraft is weakly captured for at least 50 days. The red area (dark grey) indicates trajectories which are neither bound when propagating forward nor backward. The black and white areas show true anomalies which are ruled out because the spacecraft has to be already in a bound orbit ('Incoming: closed'). The initial capture orbit is 400 x 180 000 km.

transfer delta-V and with small recovery manoeuvres in case the orbit insertion would fail.

The best solution that was found is now described. The arrival date is 5 January 2017 when the true anomaly of Mercury is 66.4°. The spacecraft position is propagated backward until it is far outside the sphere of influence of Mercury and far beyond the Lagrange point. This heliocentric state vector is then matched with a transfer trajectory which is calculated using the trajectory optimisation tool DITAN [4].

3. INTERPLANETARY TRANSFER TRAJECTORY

The transfer trajectory is nearly identical to the "hyperbolic-approach" scenario up to the second Mercury flyby: The launch into a parking orbit takes place on 13 April 2012. The spacecraft leaves the Earth-Moon system after a lunar flyby on 25 June 2012. On 1 Nov 2013 there is an Earth flyby followed by two Venus flybys on 27 Mar and 7 Nov 2014. Then 4.5 heliocentric orbits with long thrust arcs bring the spacecraft to its first Mercury flyby on 30 June 2016 and half a Mercury year later to its second Mercury flyby on 10 Aug 2016 [6]. The difference starts here: To approach Mercury through the Lagrange L1 point of the Sun-Mercury system, the second Mercury flyby needs to be performed over the midday side of Mercury rather than over midnight. The spacecraft is slung initially outside Mercury's orbit and

one long braking arc is required (once the spacecraft is inside Mercury's orbit) to achieve the right energy level for the gravitational capture. Nominal Mercury orbit insertion (MOI) is foreseen on 5 January 2017 (Mercury is then 15.7 deg to the "right" of the Sun as seen from the Earth). Table 2 gives the details of this trajectory and Fig. 2 shows this trajectory projected onto the ecliptic plane.

Table 2. Main characteristics for the trajectory with gravitational capture (delta-V numbers in brackets are without navigation and 5 % margin). A chemical motor is used to transfer the spacecraft from the initial capture orbit to the MMO orbit (400 x 12 000 km).

Departure		
Launch	13-04-2012	(MJD2000: 4486)
Moon Flyby	25-06-2012	(MJD2000: 4559)
Arrival		
Date	05-01-2017	(MJD2000: 6214.9)
$v_{periherm}$	3.908 km/s	
Arg. of periherm	178°	
β angle	0°	
Cruise time	4.73 years	(1729 days)
Mass		
Initial	2155 kg	
Final	1092 kg	
Consumption	Propellant	Delta-V
Low-thrust	356 kg	8.21 (7.13 km/s)
Chemical	131.8 kg	0.352 (0.311 km/s)
Solar-electric propulsion module		
Dry mass	560 kg	
Max. thrust	400 mN	
Total impulse	16.1 MNs	

The thrust profile is shown in Fig. 3 by the blue (solid) curve. It is assumed that the spacecraft is equipped with three 200 mN thrusters. When little power is available (outside the orbit of Venus) one thruster is on, when more power is available two thrusters can work at the same time. The third thruster is for redundancy. Fig. 3 also shows the thrust profile of the hyperbolic approach. It can be seen that a bit more thrusting is required at the very last part of the trajectory in order to further reduce the hyperbolic excess velocity. The increase in interplanetary delta-V is about 190 m/s. However it must be mentioned that the arrival conditions in the hyperbolic approach do not fulfill the requirements for the target argument of periherm and right ascension of ascending node. To adjust these orbital elements 140 m/s are required. Thus the interplanetary delta-Vs are nearly identical.

Figs. 4 and 5 show the thrust angles (describing the thrust direction) as function of time. The "angle-of-attack" is the angle between the thrust vector and its projection on the local tangential plane. It gives the in-orbit-plane component of the thrust vector. A positive angle-of-attack indicates the thrust vector pointing outside, a negative angle-of-attack pointing inside the orbit of the spacecraft. The "side-slip angle" is the angle between

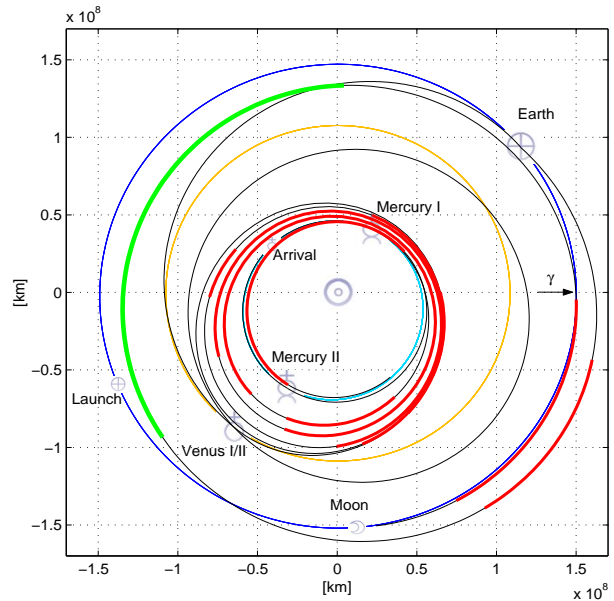


Figure 2. Optimum interplanetary trajectory of Bepi-Colombo with a gravitational capture in Jan 2017. Red (thick) lines show the arcs where the spacecraft is braking, the second thrust arc (green line on the left) shows the only accelerating arc.

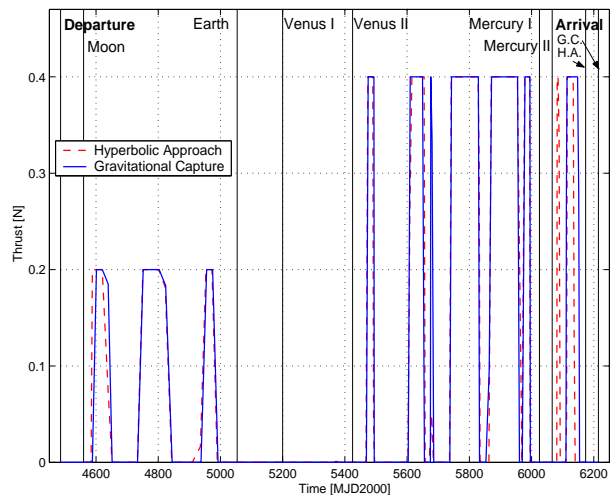


Figure 3. Thrust level for the transfer with a gravitational capture compared with the "traditional" thrust profile.

the projection of the thrust vector on the local tangential plane and the velocity vector. It gives the out-of-orbit-plane component of the thrust vector. A side-slip angle of around 0° corresponds to an accelerating thrust arc, a side-slip angle of around 180° to a braking thrust arc. The thrust angles are set to zero during coast arcs.

4. SIMULATION: FAILED ORBIT INSERTION

The spacecraft arrives from interplanetary space with a very low excess velocity and from a direction where the

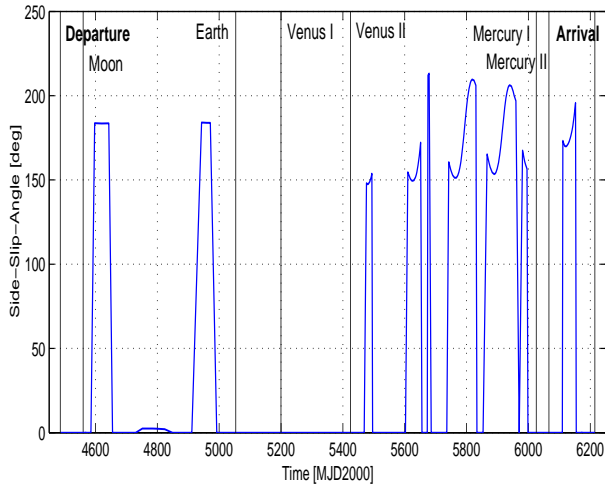


Figure 4. Side-slip angle (out-of-plane component) of the thrust vector as function of time for the transfer with a gravitational capture in Jan 2017.

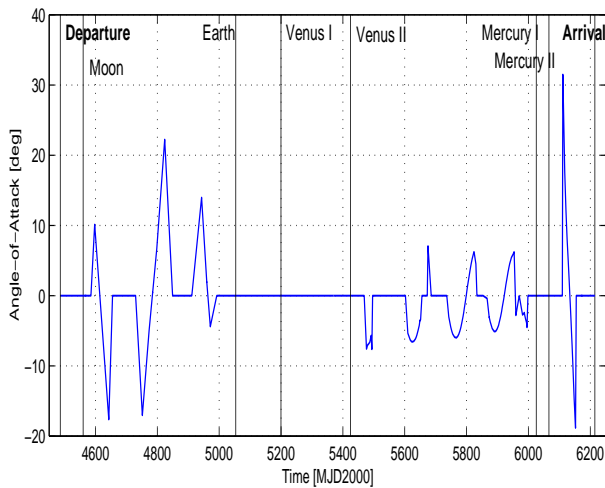


Figure 5. Angle-of-attack (in-plane component) of the thrust vector as function of time for the transfer with a gravitational capture in Jan 2017.

gravity of Sun and Mercury have similar effects on the orbit. These effects can be exploited to capture the spacecraft into a highly eccentric orbit without orbit insertion manoeuvre. The approach trajectory passes close to the L1 point of the Sun-Mercury system as seen in Fig. 6.

This approach trajectory was specifically chosen such that the Sun perturbations guarantee a temporarily stable orbit: If the orbit insertion on 5 Jan 2017 fails, the spacecraft will make 5 revolutions around Mercury before escaping again. Fig. 7 which is a close-up of Fig. 6 illustrates the trajectory evolution solely determined by Sun and Mercury gravity.

Table 3 shows the osculating orbital elements at the following pericentre passages if no manoeuvres were performed. It can be seen that at the second, fifth and sixth periherm, the altitude, inclination and orientation of the

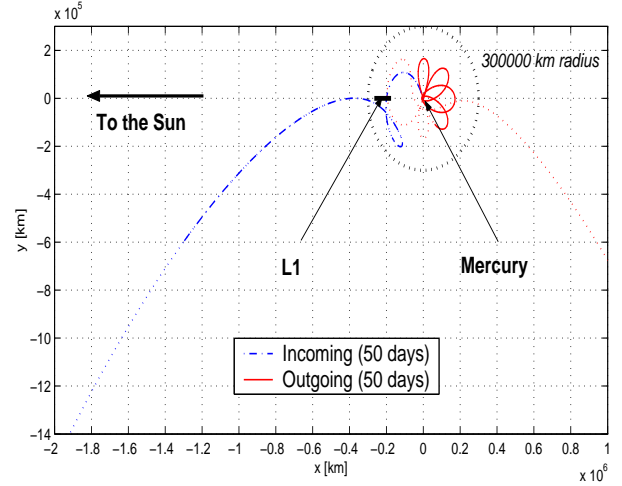


Figure 6. Ballistic arrival trajectory of the gravitational capture in a co-rotating reference frame (osculating capture orbit: 400 x 180 000 km).

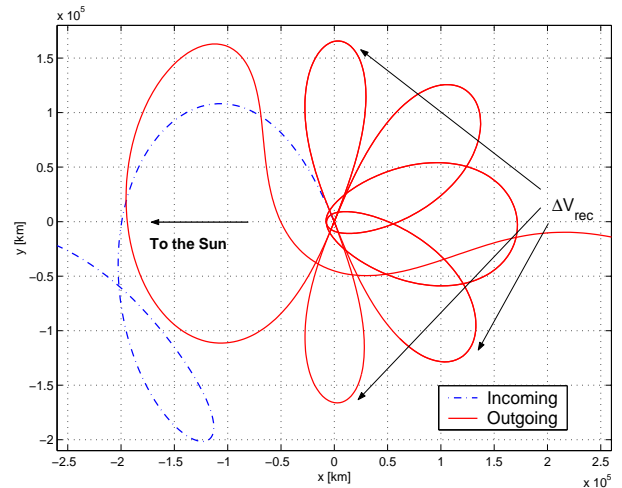


Figure 7. Ballistic arrival trajectory of the gravitational capture in a co-rotating reference frame (close-up of previous figure). ΔV_{rec} indicates the possible recovery manoeuvres in case the orbit insertion fails.

line of apsides is not very far from the nominal values. Changing the orbits with small manoeuvres (ΔV_{rec} less than 10 m/s) close to the previous apoherms new orbit insertion possibilities arise with nearly the same orbital parameters. Also the Mercury true anomalies are in the allowed limits of $\pm 60^\circ$ to 120° . These are the reasons why this particular trajectory was selected amongst the many possible solutions.

5. APPROACH NAVIGATION

Having found a trajectory that does not cost more in terms of interplanetary ΔV , has a lower orbit insertion ΔV and provides ample opportunities to recover from an orbit insertion failure, the next imminent question was the safety aspect. The main challenge to fly around the Lagrange point and to exploit the Sun gravitation for capture is the

Table 3. Osculating orbital elements after a failed orbit insertion and corresponding Δ for a recovery manoeuvre.

	2nd Periherm	3rd Periherm	4th Periherm	5th Periherm	6th Periherm
Time from failure [day]	11.4	24.9	39.1	52.4	63.9
Mercury true anomaly	115.49	158.26	-162.21	-121.14	-73.9
Periherm altitude [km]	442	5118	4541	47	0
Inclination	90°	140°	139°	90°	90°
Argument of periherm	176°	177°	186°	186°	184°
β	3.3°	-1.30°	-3.6°	-10.0°	-6.9°
ΔV_{rec} [m/s]	1	100*	100*	3	5

* order of magnitude

navigation of the spacecraft. Hence the orbit determination and correction is analysed to demonstrate that this kind of capture is actually feasible and operationally not too complex.

Figs. 8 and 9 show the last 60 days before the nominal orbit insertion. Except for the trajectory correction manoeuvres (TCM) this part of the trajectory is purely ballistic. A detailed navigation analysis of this part of the trajectory is presented in [8]. Table 4 gives the dates and magnitudes of the correction manoeuvres. Three correction manoeuvres are scheduled: the first one 50 days before arrival (MOI-50), the second one 22 days before (MOI-22) and the third one 6 days before (MOI-6). Under the assumptions described in [8], in 99 % of the Monte Carlo runs, 10 m/s will be sufficient to navigate to the targeted orbit insertion position. However, if e.g. the initial velocity uncertainty is larger than the assumed 1 m/s in all three coordinates, the first correction manoeuvre will increase. Therefore it is proposed to allocate 30 m/s in the approach navigation delta-V budget. Table 5 shows the evolution of the 1σ dispersion ellipsoid at periherm. Since the semi-major axis (SMA) of the radial/cross-track error ellipse is very close to the radial direction after TCM₃ (θ close to 0°), the precision in the pericentre altitude will be plus/minus 9 km (3σ value).

Table 4. Trajectory correction manoeuvres Δv statistics.

	Day	MJD2000	Δv [m/s]		
			Mean	95%	99%
TCM ₁	MOI-50	6164.9	2.001	3.869	4.682
TCM ₂	MOI-22	6192.9	0.698	1.667	2.183
TCM ₃	MOI-6	6208.9	0.830	1.913	2.505
Total	—	—	3.529	7.449	9.370

It was also shown in [8] that regular momentum wheel off-loading manoeuvres, occasional 2-day communication blackouts (even around critical dates) and safe modes with a residual net delta-V of 0.5 m/s in an unknown direction will not jeopardise the approach navigation. All contingency cases which were simulated could be handled with small (less than 10 m/s) delta-V penalties. The positional dispersion ellipsoid at the periherm after the last TCM never intruded altitudes below 380 km.

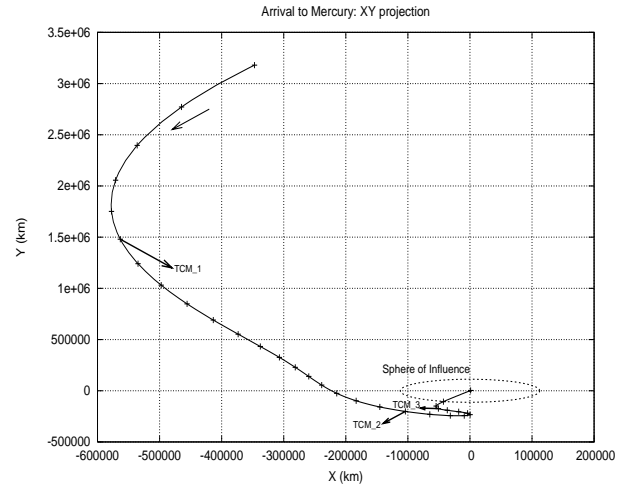


Figure 8. Ballistic arrival trajectory of the gravitational capture (XY projection in a Mercury reference frame). Tick marks are drawn every 2 days. The directions of the correction manoeuvres are not representative.

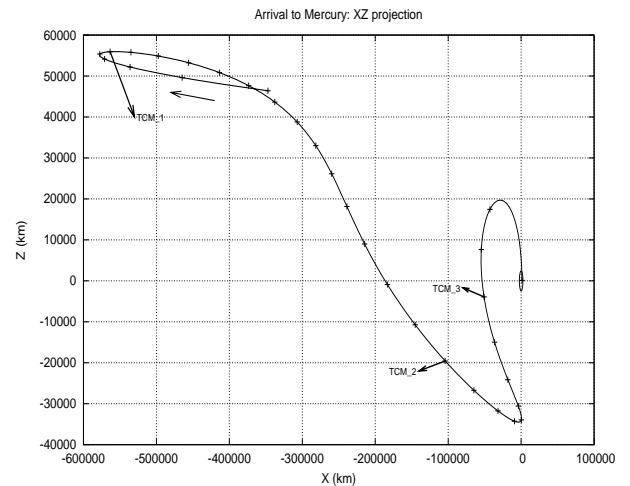


Figure 9. Ballistic arrival trajectory of the gravitational capture (XZ projection in a Mercury reference frame). Tick marks are drawn every 2 days. The directions of the correction manoeuvres are not representative.

6. CONCLUSIONS

A new orbit insertion strategy at Mercury was analysed where the Sun perturbations are exploited to get weakly captured into a Mercury orbit. The solar electric propul-

Table 5. 1σ dispersion ellipsoid at perihelion before and after the trajectory correction manoeuvres. SMA is the semi-major axis of the radial/cross-track error ellipse, SmA the semi-minor axis, θ is the angle between the semi-major axis and the radial direction and LTOF is the linearised-time-of-flight error, i.e. the along-track error.

	MJD2000 (wrt MOI)	SMA [km]	SmA [km]	θ [deg]	LTOF [s]
TCM ₁ ⁻	6164.9	1484.068	146.081	-41.324	591323.107
TCM ₁ ⁺	(MOI-50)	63.178	8.401	-35.048	22353.108
TCM ₂ ⁻	6192.9	69.217	8.995	-35.861	24978.492
TCM ₂ ⁺	(MOI-22)	8.565	1.184	-6.411	971.673
TCM ₃ ⁻	6208.9	8.892	1.607	-7.586	1221.332
TCM ₃ ⁺	(MOI-6)	3.091	0.152	1.319	13.890

sion requirements during interplanetary cruise are the same as in a hyperbolic approach, but the orbit insertion manoeuvre is considerably smaller because of the lower arrival velocity. The main advantage, however, of this scenario is the failure tolerance of the chemical insertion burn: There are approach geometries where correction manoeuvres of less than 10 m/s exist which will bring the spacecraft back to the desired perihelion conditions after one or even several orbit insertion failures.

A detailed navigation analysis showed that the orbit determination and control of the spacecraft around the Lagrange point is not more complex than in a hyperbolic approach. Therefore, the gravitational capture at Mercury can even be considered as the safer option.

ACKNOWLEDGEMENTS

The authors thank Vicente Companys, Martin Hechler, Mike McKay, Trevor Morley, Johannes Schoenmaekers and Zeina Mounzer for their very useful advice during the navigation analysis.

REFERENCES

[1] Belbruno, E., Lunar Capture Orbits, a Method of Constructing Earth Moon Trajectories and the Lunar Gas Mission, AIAA-87-1054, 19th AIAA/DGLR/JSASS International Electric Propulsion Conference, Colorado Springs, USA, 1987.

[2] Belbruno, E. and Miller, J., A Ballistic Lunar Capture Trajectory for the Japanese Spacecraft Hiten, *JPL IOM 312/90.4-1731*, 1990.

[3] Belbruno, E. and Miller, J., Sun-Perturbed Earth-to-Moon Transfers with Ballistic Capture, *Journal of Guidance, Control and Dynamics*, Vol. 16, No. 4, pp. 770-775, 1993.

[4] Bernelli-Zazzera, F., Vasile, M., Fornasari, N. and Masarati, P., Design of Interplanetary and Lunar Missions Combining Low Thrust and Gravity Assists, *Final Report of ESA/ESOC contract No. 14126/00/D/CS*, Sept. 2002.

[5] Campagnola, S., Jehn, R. and Corral, C., Design of Lunar Gravity assist for the BepiColombo Mission to Mercury, 14th AAS/AIAA Space Flight Mechanics Conference, Maui, Hawaii, AAS 04-130, 8-12 Feb. 2004.

[6] Campagnola, S., Garcia, D., Jehn, R., Corral, C. and Croon, M., BepiColombo Mercury Cornerstone Mission Analysis: Soyuz/Fregat Launch in 2012, *MAO Working Paper 466*, Draft 1.3, September 2004.

[7] Carusi, A. and Valsecchi, G., Numerical simulation of close encounters between Jupiter and minor bodies, *Asteroids*, Univ. Az. Press, Tucson, pp. 391-416, 1979.

[8] Garcia, D., Jehn, R. and Sánchez, N., BepiColombo Mercury Cornerstone Mission Analysis: Orbit options, Radio Science and Guidance Analysis, *MAO Working Paper 476*, Draft 1.1, September 2004.

[9] Jehn, R., Corral, C. and Giampieri, G., Estimating Mercury's 88-day libration amplitude from orbit, *Planetary and Space Science*, Vol. 52, pp. 727-732, 2004.

[10] Kemble, S., Interplanetary Missions Utilising Capture and Escape Through the Lagrange Points, IAC-03-A.1.01, 54th International Astronautical Congress, Bremen, Germany, 29 Sep. - 3 Oct. 2003.

[11] Koon, W.S., Lo, M.W., Marsden, J.E. and Ross, S.D., Resonance and capture of Jupiter comets, *Celestial Mechanics and Dynamical Astronomy*, 81(1-2), pp. 27-38, 2001.

[12] Ross, S.D., Statistical theory of interior-exterior transition and collision probabilities for minor bodies on the solar system, in *Libration Point Orbits and Applications* (Eds. G. Gomez, M.W. Lo and J.J. Masdemont), World Scientific, pp. 637-652, 2003.

[13] Yamakawa, H., Kawaguchi, J., Ishii, N. and Matsuo, H., On Earth-Moon Transfer Trajectory with Gravitational Capture, AAS 93-633, AAS/AIAA Astrodynamics Specialist Conference, Victoria, USA, 16-19 Aug. 1993.